Single Source Precursors for Calcium Sulfide (CaS) Deposition

P. S. Kubiak[a], A. L. Johnson,[a]* P. J. Cameron,[a] and Gabriele Kociok-Köhn[b]

Abstract: Here we describe preliminary studies into the synthesis structural characterisation and thermal properties of a family of calcium xanthate precursors for application in the deposition of CaS thin films. The straightforward, low-temperature syntheses are detailed along with characterisation of the resulting compounds by ^{1}H and ^{13}C NMR and elemental analysis. Solid state molecular structures of all compounds, obtained from single-crystal X-ray diffraction, are presented and discussed in detail. The decomposition behaviour of the precursors has been probed through TGA, TGA-MS and thermal annealing experiments, indicating that the compounds decompose cleanly into CaS.

Introduction

Alkaline-earth sulfides (MgS, CaS, SrS and BaS) have been the subject of interest both theoretically[1] and experimentally[2] for some time now, and are the most widely studied as materials for emissive layer matrices in thin-film electroluminescent (TFEL) displays, including cathode-luminescence,[3] electro-luminescence[4] and photo-luminescence.[4a, 4b, 5] As pure materials, however, these binary sulphides are incapable of luminescence, and it is only when doped with other elements that these properties are exhibited. To this end, a wide variety of dopants have been used, including Ag,[4b] Bi,[5d] Cd,[4d] Ce,[5a, 6] Cu,[3b, 4a, 4b, 5f], Eu,[4c, 4e, 4f, 5b, 5c, 5g, 6b, 7] Pb,[3b, 5e, 8] Sb,[9] Si,[10] Sm,[5b, 5c, 7b] Tb[6] and Tm.[11] Perhaps not unsurprisingly the most abundant of the alkaline earth metal sulphides, *i.e*. CaS, is the most widely studied, and has found a new niche, taking advantage of its photo-luminescent properties to act as a phosphor in phosphor converted white LEDs[3a, 7a] and IR up-conversion.[5c, 7b]

Whilst CaS is most commonly deposited as a thin film, the properties of CaS quantum dots have also been investigated.[5a, 12] In the vast majority of cases, these thin films have been deposited by batch-process techniques, including ALD,[1b, 6, 7d, 8, 10, 12-13] CVD,[14] e-beam evaporation,[4a, 4b, 5d-f, 7b] magnetron sputtering[5c, 7b, 11] and PLD.[7c] While, these processes are effective at producing high quality, controllable films, they are not easily scalable, suffering from not only unavoidable issues of toxicity (H_2S) but also inconveniently low precursor volatility which in turn necessitates the use of high vacuum methods.

An alternative variant on these techniques, which circumvents this latter limitation, and avoids the use of toxic H_2S, is aerosol-assisted CVD (AA-CVD).[15] For AA-CVD the only restriction on precursor identity is its solubility in an appropriate solvent, which may be nebulised and the solution transported as micron-scale droplets to a heated substrate.

Whilst routes towards the deposition of Group 2 metal sulfides have been explored using dual source CVD including the calcium precursor (M(β-diketonate)$_2$ (Fig. 1a) and H_2S[10] or ^{t}BuSH,[16] [Ca_3(thd)$_6$] and H_2S,[17] and ALD ([Ca(thd)$_2$(tetraen)] (Fig. 1b) and H_2S,[13a] or [{RC(N^{i}Pr)$_2$}$_2$Ca}$_2$] (R = H or Me)[1b] (Fig.1c) and H_2S. To our knowledge, only one single source precursor for the production of CaS thins films has been reported to date. The non-volatile crown-ether derivative [(15-crown-5)·Ca(SOCMe)$_2$] (fig. 1d) has been employed as single source precursor for the AA-CVD of CaS, which displayed preferential orientation (200) CaS, at 310 °C.[18]

This dearth of precursors has prompted us to investigate the application of xanthate ligands to group 2 metal chemistry with particular focus on the synthesis and application of calcium xanthate systems and single source precursor for the production of CaS thin films. Metal xanthates complexes, have found application in the formation of a range metal sulphide materials e.g. ZnS,[19] CdS[20] PbS[21] CuS[22] and NiS,[23] with the xanthate ligands providing a highly selective pathways to metal sulfide formation via the low temperature Chugaev elimination reaction, in which alkene (R–H), OCS and MSH fragments are formed. Even more significantly the decomposition of these materials can be some 100 °C, or more, lower than the analogous dithiocarbamates.[24] To this end we describe here, primary results concerning the synthesis, characterisation, structural studies and thermal behaviour of a family of calcium xanthate complexes.

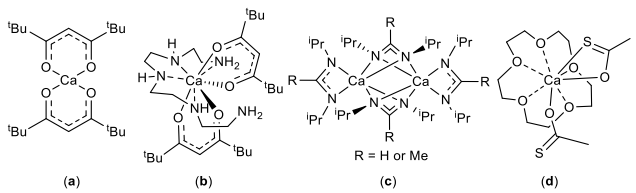

Figure 1. Previously reported duel source CVD (**a**), LP-CVD (**b**), ALD (**c**) and only single source AA-CVD precursors (**d**) for CaS formation reported to-date.

[a] Dr Peter S. Kubiak, Prof. Andrew L. Johnson and Prof. Petra J. Cameron
Department of Chemistry
University of Bath
Claverton Down, Bath, BA2 7AY. UK.
E-mail: a.l.johnson@bath.ac.uk
Homepage: https://aljohnson58.wixsite.com/andrewjohnsongroup
[b] Dr. Gabriele Kociok-Köhn
Materials and Chemical Characterisation (MC^2) Facility
University of Bath
Claverton Down, Bath, BA2 7AY. UK.

Results and Discussion

Synthesis and Characterisation

The direct synthesis of metal xanthate complexes is possible by reacting CS_2 with an alcohol, which is also used a solvent, in the presence of base (e.g. KOH) and an appropriate metal reagent. The direct insertion of CS_2 into the M-O bonds of metal alkoxides provides an alternative and salt free route to metal xanthate complexes where suitable metal alkoxides and phenoxides exist. In the case of calcium, Mingos and co-workers have previously reported the synthesis of Ca alkoxides by the direct reaction of calcium metal with either ethanol or isopropanol.[25] Whilst subsequent reaction with CS_2 was shown to result in the formation of the corresponding ethyl and isopropyl xanthates their molecular structure were not elucidated, nor were their potential for the deposition of CaS explored.

Reaction of Ca metal with dry ethanol results in the formation of the corresponding solvated calcium *bis*-ethoxide system [{$Ca(OEt)_2(ROH)_3$}] as has been reported previously.[25] Whilst this complex is not of sufficient stability or crystallinity to be structurally characterised, reaction with carbon disulphide affords an immediate colour change and formation of the *bis*-ethylxanthate complex [{$Ca(S_2COEt)_2(EtOH)_3$}] (**1**). The yellow solution was filtered in order to remove any insoluble residues and compound **1** was isolated as crystalline materials after cooling the solution to -28 °C.

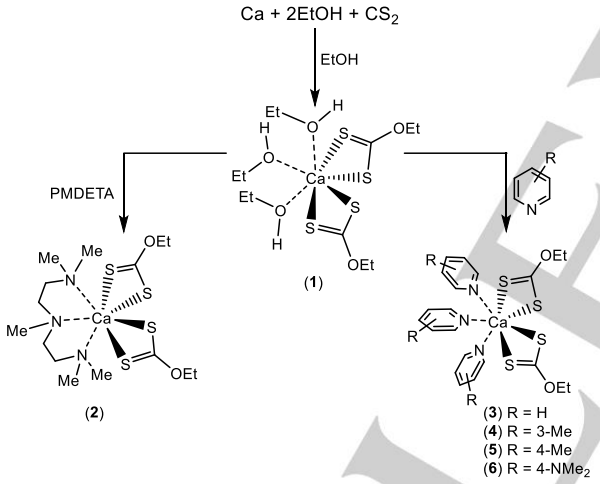

Scheme 1. Synthesis of complexes **1**-**6**.

The novel adducts **2**, **3**, **4**, **5** and **6** are all formed on a scale between 1-10g with ease, in nearly quantitative yield, by reacting complex **1** with the ligands PDMAT, pyridine, 3-methyl-pyridine, 4-methyl-pyridine and 4-dimethylamino-pyridine respectively (Scheme 1). The complexes are soluble in chloroform, dichloromethane, tetrahydrofuran and toluene, and were easily purified by recrystallization from toluene solutions. The ^1H and ^{13}C NMR data for these compounds are unexceptional and confirm their composition, but shed little light on the solid-state structures, *i.e.* the presence of terminal or bridging xanthate groups. In the case of complex **1**, the ^1H NMR spectra consists of resonances for the {S_2COEt} group at δ 1.14 and 4.57 ppm as well as resonances associated with coordinated {EtOH} groups at, δ 1.03, 2.26 and 3.57 ppm, for the {CH_3} {OH} and {CH_2} groups respectively, as previously reported.[25]. These resonances, in a relative ratio of 3:2, are consistent with a formulation of [{$Ca(S_2COEt)_2(EtOH)_3$}], confirmed by elemental analysis.

The ^1H NMR spectra of compound **2** consists of the expected resonances for the {S_2COEt} groups at, δ 1.10 and 4.64 ppm respectively. Additionally, the {NMe_2} and {NMe} peaks from the PMDTA ligand are present at δ 2.18 and 2.35 ppm, with integrals for these resonances consistent with a compound formulation of [{$Ca(S_2COEt)_2$(PMDTA)}].

For the pyridine dervatized complexes, **3**-**7** the ^1H NMR spectra indicate the pyridine ligands to be in a 3:2 ratio with the xanthate groups, retaining the core calcium moiety, [{$Ca(S_2COEt)_2$}]. No significant change in the resonances attributed to the {CH_3} and {CH_2} moieties [δ = 1.11-1.15 and 4.61-4.66 ppm] was observed for complexes **3**, **4** and **5**. Similarly, the DMAP-containing complex **7** similarly demonstrated relatively straightforward ^1H and ^{13}C NMR spectra, and while a small change in the ^1H NMR chemical shift of the {S_2COEt} is observed, with resonances shifting to slightly higher values of δ = 1.21 {CH_3} and 4.76 {CH_2} ppm. Unfortunately, low-temperature solution state NMR studies were unable to provide more exacting information concerning the structure of these complexes. Satisfactory elemental analysis were obtained in all cases confirming the formation of complexes of the general form [{$Ca(S_2COEt)_2(Py)_3$}]. Full ^1H and ^{13}C NMR spectra for complexes **2**-**6** are reported in the supporting information. Attempts to further characterize **2-6** by ESI-MS was impaired by their low thermal stability (vide infra).

Molecular structures:

[{$Ca(S_2COEt)_2(EtOH)_3$}] (1): While characterisation data for this compound has previously been reported[25] its solid state structure has not. X-ray single crystal analysis confirms the insertion of CS_2 into both Ca-OEt bonds of the intermediate calcium ethoxide. The solid-state molecular structure of **1** is shown in Figure 2 along with selected bond lengths and bond angles.

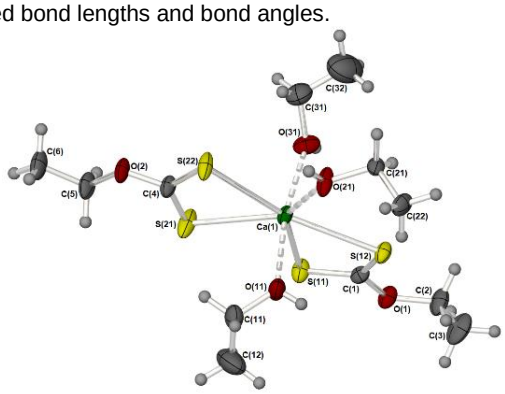

Figure 2. Molecular structure of complex **1**, including selected bond lengths (Å) and bond angles (°). Bond lengths: Ca(1)-S(11) 2.9095(7); Ca(1)-S(12) 2.9361(6); Ca(1)-S(21) 2.3695(15) ; Ca(1)-S(22) 2.9133(6) ; Ca(1)-O(11) 2.3471(15); Ca(1)-O(21) 2.3695(15); Ca(1)-O(31) 2.3278(16); S(11)-C(1) 1.6874(19); S(12)-C(1) 1.692(2); O(1)-C(1) 1.339(2); O(1)-C(2) 1.447(3); S(21)-C(4) 1.680(2); S(22)-C(4) 1.697(2); O(2)-C(4) 1.339(2); O(2)-C(5) 1.457(2). Bond Angles: S(11)-Ca(1)-S(12) 61.178(16); S(21)-Ca(1)-S(22) 61.342(16); S(11)-C(1)-S(12) 123.34(11); S(21)-C(4)-S(22) 123.27(11); S(11)-Ca(1)-S(21) 77.383(18); S(12)-Ca(1)-S(22) 160.23(2); O(11)-Ca(1)-O(21) 88.46(6); O(21)-Ca(1)-O(31) 88.13(6); O(11)-Ca(1)-O(31) 170.79(6). Thermal ellipsoids are shown at 50% probability.

The solid-state molecular structure of **1** is shown in Figure 1 along with selected bond lengths and bond angles. The complex, **1**, which is isostructural to the previously reported isopropyl derivative [{Ca(S_2CO^iPr)$_2$(^{i}PrOH)$_3$}],[25a] consists of a seven-coordinate calcium atom, bound to the four sulphur atoms of the two xanthate groups, {S_2COEt}, as well as the oxygen atoms of three coordinating molecules of ethanol. As such, the coordination geometry about the calcium atom is best described as pentagonal bipyramidal, with two EtOH groups in axial positions. The two bidentate xanthate ligands [mean S-Ca-S 61.26°] display different coordination geometries: one ligand is bonded symmetrically [Ca(1)-S(21) 2.913(1), Ca(1)-S(22) 2.913(1)]. The second xanthate is bound asymmetrically, having one short and one longer Ca-S interaction [Ca(1)-S(11) 2.909(1), Ca(1)-S(12) 2.936(1)]. The equatorial Ca-O distance [Ca(1)-O(21) 2.3695(15)] is longer than the two axial EtOH distances [Ca(1)-O(11) 2.3471(15), Ca(1)-O(31) 2.3278(15)].

[{Ca(S_2COEt)$_2$(PMDTA)$_3$}] (2): The solid-state structure of compound **2**, shown in Figure 3, shown the presence of a uni-molecular complex which incorporates a tridentate PMDETA ligand, binding to the Ca centre in a κ^3-coordination mode. The additional coordination by four sulphur atoms, of the two distinct xanthate groups results again in a seven-coordiatate Ca centre, and is reminiscent of the *iso*-formulaic Pb complex [{Pb(S_2COEt)$_2$(PMDTA)}].[26] For the two xanthate groups, the one involving O(2) is largely symmetrically bound [Ca–S: 2.9035(13), 2.9199(12) A˚] whilst the other xanthate ligand, based on O(1), binds more asymmetrically with one long Ca-S and one shorter CaS interaction [Ca–S: 2.8157(9), 2.9351(10) Å].

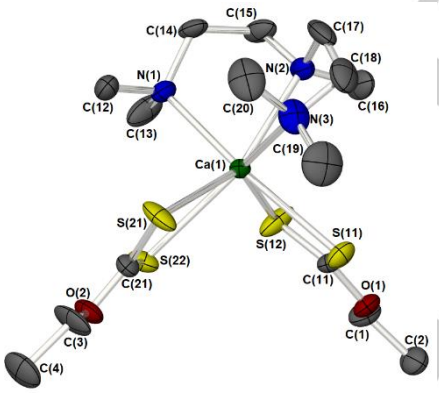

Figure 3. Molecular structure of complex **2**, including selected bond lengths (Å) and bond angles (°). Bond lengths: Ca(1)-S(11) 2.8157(9); Ca(1)-S(12) 2.9351(10); Ca(1)-S(21) 2.9035(13); Ca(1)-S(22) 2.9199(12); Ca(1)-N(1) 2.525(2); Ca(1)-N(2) 2.612(2); Ca(1)-N(3) 2.599(3); S(11)-C(11) 1.688(3); S(12)-C(11) 1.682(3); O(1)-C(11) 1.340(3); O(1)-C(1) 1.442(4); S(21)-C(21) 1.663(5); S(22)-C(21) 1.708(6); O(2)-C(21) 1.317(5); O(2)-C(3) 1.447(7). Bond Angles: S(11)-Ca(1)-S(12) 62.55(2); S(21)-Ca(1)-S(22) 61.00(4); S(11)-Ca(1)-S(21) 102.76(4); S(11)-Ca(1)-S(22) 94.85(3); S(12)-Ca(1)-S(22) 74.30(4); S(12)-Ca(1)-S(21) 131.90(4); N(1)-Ca(1)-N(2) 71.14(8); N(1)-Ca(1)-N(3) 108.94(9); N(2)-Ca(1)-N(3) 70.21(9). Thermal ellipsoids are shown at 50% probability. Hydrogen atoms have been omitted for clarity.

[{Ca(S_2COEt)$_2$(Py)$_3$}] (3), [{Ca(S_2COEt)$_2$(3-Me-Py)$_3$}] (4), [{Ca(S_2COEt)$_2$(4-Me-Py)$_3$}] (5) and [{Ca(S_2COEt)$_2$(4-Me$_2$N-Py)$_3$}] (6): Compounds **3**, **4**, **5** and **6** are isostructural and as such discussion is restricted to **3** an example. Figure 4 shows the solid-state molecular structures of compounds **3**, **4** and **6**, whilst selected bond lengths and angles are presented in Table 1. The molecular structure of **5** is shown in the supporting information. In all four cases (**3**-**5**), single crystal X-ray diffraction analysis reveals the solid state structures to comprise of seven coordinate Ca centres supported by four equatorially positioned sulphur atoms, of the two xanthate ligands and three nitrogen atoms of the pyridine based ligands (two axial and one equatorial) in what is best described and a pentagonal pyramidal arrangement, similar to complex **1**. The Ca-N distances shown in Table 1 are fully consistent with previously reported Ca-pyridine/phenanthroline complexes.[27] Bond lengths and angles shown in Table 1 are relatively consistent across complexes **3**-**6** and in general are the same within the error limits.

Table 1. Selected bond lengths (Å) and angles (°) for complexes **3**-**6**

Complex:	**3**	**4**	**5***	**6**
		Bond lengths (Å)		
Ca-N(101)	2.5144(15)	2.5150(18)	2.491(4)	2.4942(18)
Ca-N(301)	2.4958(16)	2.5320(16)		2.4942(18)
Ca-N(201)	2.5705(15)	2.5351(19)	2.567(4)	2.5044(17)
Ca-S(11)	2.9186(6)	2.9028(6)	2.8954(8)	2.9480(7)
Ca-S(12)	2.8800(6)	2.9023(7)	2.9127(12)	2.9631(7)
Ca-S(21)	2.9039(6)	2.8815(9)		2.9196(7)
Ca-S(22)	2.9024(6)	2.8966(6)		2.8998(7)
S(11)-C(11)	1.6806(18)	1.681(2)	1.691(4)	1.692(2)
S(12)-C(11)	1.6927(19)	1.679(2)	1.670(4)	1.678(2)
S(21)-C(21)	1.672(2)	1.695(3)		1.695(2)
S(22)-C(21)	1.6985(19)	1.689(3)		1.683(2)
O(1)-C(11)	1.335(2)	1.349(3)	1.335(4)	1.346(3)
O(2)-C(21)	1.340(2)	1.334(3)		1.334(3)
		Bond Angles (°)		
N(101)-Ca-N(301)	175.60(5)	174.19(6)	174.79(14)	171.21(6)
N(101)-Ca-N(201)	91.65(5) 92.74(5)	85.40(6) 89.68(6)	87.40(7)	88.93(6) 83.88(6)
N(201)-Ca-N(301)				
S(11)-Ca-S(12)	61.845(15)	61.399(17)	61.56(3)	60.582(18)
S(21)-Ca-S(22)	61.723(16)	62.27(2)		61.666(18)
N(201)-Ca-S	S(12): 76.77(3) S(22): 77.66(4)	S(21): 80.77(4) S(11): 79.02(4)	S(11): 79.03(2)	S(11): 78.02(5) S(21): 84.25(5)
S-Ca-S	82.227(17)	76.71(2)	78.82(5)	75.673(19)

* The molecular structure of **5** is shown in the supplementary information.

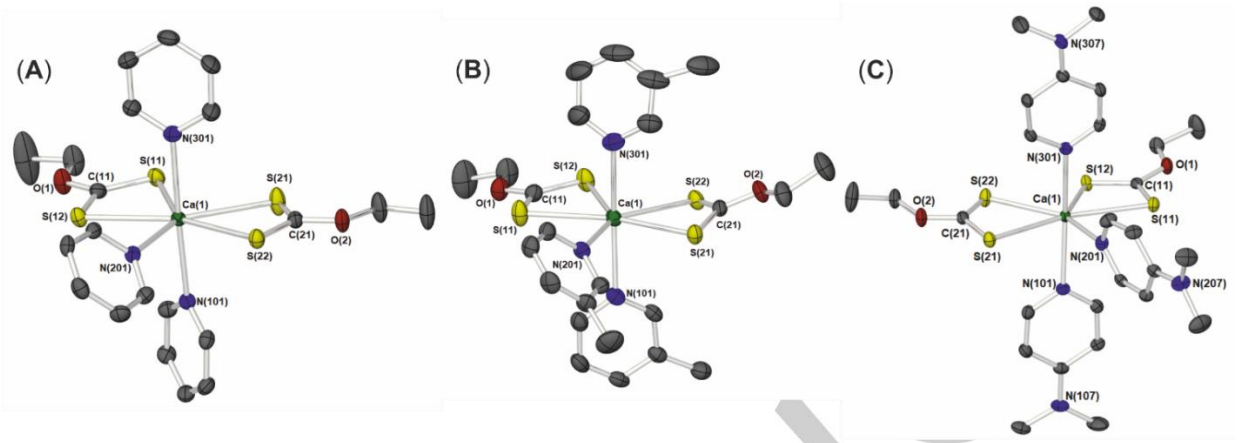

Figure 4. Solid state molecular structures of complexes **3, 4** and **6**, including selected bond lengths (Å) and bond angles (°).Thermal ellipsoids are shown at 50% probability. Hydrogen atoms have been omitted for clarity.

The small degree of asymmetry observed in **3** between equatorial [Ca-N(201) 2.571(1) and axial Ca-N interactions [Ca-N(101) 2.514(1) Å; Ca-N(301) 2.495(1) Å] is reflected in the other complexes of this series, and most likely the result of ligand packing effects.

Similarly, the Ca-S distances are very similar to each other Ca-$S_{(av)}$ 2.901 Å], with bite angels of 61.845(15)° and 61.723(16)°. It is perhaps noteworthy that whilst the Ca-N(DMAP) distances [Ca(1)–$N_{(ax)}$ 2.4942(18) Å, and Ca(1)–N(eq) 2.5044(17) Å] observed in **6** are slightly shorter than the Ca–N(py) distances in **3**, there are no structural differences. Similar observations have been made previously for Ca-N interactions in calcium-pyridine and DMAP adducts.[28]

Thermal analysis:

Thermogravimetric analysis (TGA) of complexes **1**-**6** were performed in order to gain insight into relative volatilities and thermal stabilities (Figure 5). Table 2 shows onset of decomposition temperatures as well as the % residue at 300 and 500 °C alongside the calculated residual mass for formation of $Ca(SH)_2$ and CaS respectively.These analyses were carried out with an instrument that was housed in a glove-box purge-box in order to minimize reaction with atmospheric moisture/air. As can be seen from Figure 4 compound **1** experiences an initial mass loss at approx. 55 °C which plateaus at ~240 °C (45%). A second thermal event occurs at ~313 °C with a much smaller mass loss to yield a stable residue of 34% at 500 °C. A mass residue, which is considerably higher than that expected for CaS formation (*i.e.* 17%). In contrast, complex **2** shows a significantly higher onset of decomposition (108 °C), with a rapid mass loss of 68% to yield a mass residue of 33% (at 165 °C). Between 165-308 °C the residue continues to lose mass (32% to 26%), consistent with the possible formation of $Ca(SH)_2$ as an intermediate at ~310 °C. A third thermal event occurs between 308 and 362 °C yielding a mass residue of 20%, close to the expected value of 16 % for formation of CaS.

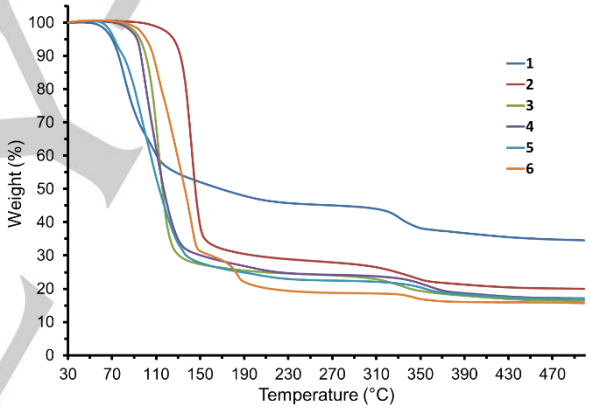

Figure 5. TGA Data for complexes **1-6**.

Table 2. Onset of volatilisation/decomposition temperature for **1**-**6**, and found and calculated % residues, at 300 °and 500 °C.

Compound	Onset Temp[§] (°C)	% Residue at 300 °C (Calc. for $Ca(SH)_2$)	% Residue at 500 °C (Calc. for CaS)
1	55	44 % (25 %)	35 % (17 %)
2	108	27 % (23 %)	20 % (16 %)
3	87	23 % (20 %)	16 % (14 %)
4	81	24 % (19 %)	17 % (13 %)
5	63	22 % (19 %)	17 %(13 %)
6	82	19 % (16) %	16 % (11 %)

[§] The temperature at which 1% mass loss has occurred

Complexes **3**-**5** share similar thermal profiles, all with an onset of decomposition between those of complex **1** and **2**., *i.e.* 87 °C (**3**), 81 °C (**4**) and 63 °C (**5**) respectively. As with complex **2** an initial mass loss of between 69 and 71% is observed, to yield mass residues of 29% (**3**), 30% (**4**) and 31% (**5**), which continue to lose

mass between (~135-310 °C) to form residues consistent with the formation of $Ca(SH)_2$. Further mass loss between 310-500 °C yields stable residues of 16% (**3**) 17% (**4**) and 17% (**5**), close to the expected values of 14 % (**3**) and 12% (**4** and **5**) for the formation of CaS. Complex **6** has a similar thermal profile compared to **3**-**5** with an onset of decomposition at 82 °C, yielding a stable residue (16%) at 500 °C, *Cf.* a calculated value of 11 % for CaS formation.

These results, while encouraging from a precursor design perspective. *i.e.* they result in the formation of the desired materials, also indicate a lack of volatility of the precursors. This lack of volatility therby limiting the application of these precursors to solution state deposition processes such as spincoating and AA-CVD.

In an attempt to ascertain possible decomposition pathways for these precursors, TGA-coupled mass spectrometry was undertaken. Unfortunately the TGA-MS experiments did not yield conclusive results with respect to precursor decomposition pathways: Peaks at *m/z* = 32 amu, *m/z* = 34 amu *m/z* = 60 amu, *m/z* = 76 amu were observed in the mass spectra which we attribute to formation of sulfur, H_2S, COS and CS_2 respectively, suggestive of a decomposition pathway similar to that described by Vreugdenhil et al.[29] The observation of H_2S is also consistant with the possible inital formation of $Ca(SH)_2$ which is capable of loss of H_2S to form CaS. We should note that peaks accociated with a Chugaev elimination process, *i.e.* m/z = 27/28 amu asociated with $\{C_2H_3\}/C_2H_4$ production were not observed.[23]

Thermal decomposition

In an imitation of the TGA process, and to demonstrate the potential application of these compounds in the formation CaS, crystals of compound **2** were placed in an annealing tube under inert argon atmosphere and heated at 400 °C for 1 hour. A powder X-ray diffraction pattern of the resulting powder is displayed in Figure 6. The diffraction peaks correspond to the, (200), (220), (222), (400) and (420) planes, which was indexed to the pure cubic phase for CaS (Oldhamite) (JCPDS File No. 75-0261, a = 0:5683 nm). Peaks relating to either CaO other phases of CaS were not detected. The broadening of the peaks indicates that the crystal sizes were small, i.e. <100 nm in size. A sample of the CaS powder produced by annealing was affixed to double-sided sticky carbon tape fixed to a flat sample holder. Attempts to aquier high resolution SEM of the powder was impeded because of excessive charging of the surface. A significant feature of this work is the air and moisture stability of the complexes developed, which are easily handled air and are very soluble in a range of common organic solvents. The thermal properties of complexes **1-4** are encouraging, displaying in general, with the exception of complex **1**, clean decomposition characteristics, all of which abrogate the use of excessively high temperatures for the deposition of metal sulfide thin films.

Conclusions

This work documents the synthesis and characterisation of a family of calcium ethyl xanthate complexes coordinated either by ethanol, PMDTA or by pyridine ligands, specifically designed for the production of CaS thin films either by AA-CVD or other suitable deposition techniques. The synthetic procedure for the calcium xanthate metal complexes is straightforward and the products can be isolated in good yields and easily produced on a larger scale.

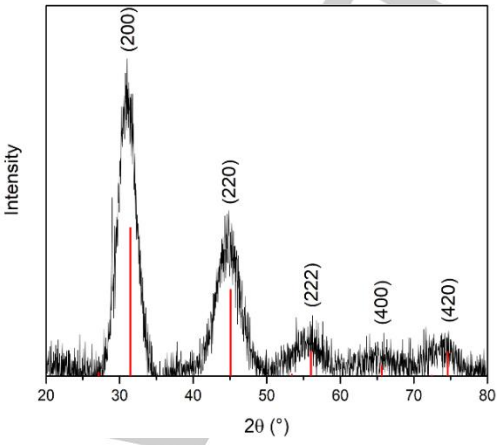

Figure 6 : PXRD patern of CaS derived from compound **2** after thermal anneling at 400 °C. Red lines show calculated peak positions and relative intesities of bulk CaS. Corresponding miller idicies are shown above the peaks.

The molecular structures of the complexes **1-6**, have been determined, revealing the metal centres to possess highly ligated 7-coordinate, coordination environments. Initial thermal investigations using the PMEDA dervatized precursor, **2**, suggest that CaS is readily formed by pyrolysis. Further work into the application of these materials in AACVD processes for the development of CaS and CaS-composite thin films (e.g. CaS-SnS) will be reported elsewhere.

Experimental Section

General procedures: Elemental analyses were performed externally by London Metropolitan University Elemental Analysis Service using an Exeter Analytical CE 440 analyser. ^{1}H, ^{13}C and ^{119}Sn NMR spectra were recorded on Bruker Advance 300 or 500 MHz FT–NMR spectrometers, as appropriate, as saturated solutions at room temperature. Chemical shifts are in ppm with respect to Me_4Si (^{1}H, ^{13}C). TGA and PXRD were performed using a Perkin Elmer TGA7 and Bruker D8 instrument (Cu-k_α radiation), respectively.TGA was collected using a TGA 4000 Perkin Elmer system. Samples were prepared air sensitively using a open aluminium sample pan. TGA's were performed under a flow of N_2 at 20 ml min^{-1} and heated from 30 °C to 600 °C at a ramp rate of 5 °C min^{-1}. Thermal decomposition experiments were carried out in a quartz tube under inert atmosphere in a tube furnace. TGA-MS was performed under argon (20 ml/min) at a ramp rate of 5 °C/min between 30 and 600 °C on a Setaram Setsys Evolution TGA 16/18 with the evolved gases passing through a Pfeiffer Vacuum Omnistar GSD 320 quadrapole mass spectrometer. Samples were contained in alumina crucibles. Experiments were performed by MC^2, University of Bath, UK, and results were analysed using Excel. All reactions were carried out under an inert atmosphere using standard Schlenk techniques. Solvents were dried and degassed under an argon atmosphere over activated alumina columns using an Innovative Technology solvent purification system (SPS). The low thermal stability of complexes **2-6** precluded the use of ESI-MS.

Table 3. Crystal and structure refinement data for **1**-**6**.

Compound reference	**1**	**2**	**3**	**4**	**5**	**6**
Chemical formula	$C_{12}H_{28}CaO_5S_4$	$2(C_{15}H_{33}CaN_3O_2S_4)$ •$0.5(C_{13}H_{14})$	$C_{21}H_{25}CaN_3O_2S_4$	$C_{24}H_{31}CaN_3O_2S_4$	$C_{24}H_{31}CaN_3O_2S_4$ •C_7H_8	$C_{27}H_{40}CaN_6O_2S_4$ •C_7H_8
Formula Mass	420.66	996.64	519.76	561.84	653.97	741.10
Crystal system	Triclinic	Triclinic	Monoclinic	Triclinic	Monoclinic	Triclinic
a/Å	10.1314(6)	8.4739(5)	16.9062(6)	8.7081(3)	9.8429(3)	11.5902(6)
b/Å	10.4347(5)	8.9288(5)	16.5621(4)	11.1043(3)	21.8577(6)	11.7287(7)
c/Å	11.6333(6)	19.1663(9)	9.5038(3)	17.1306(5)	16.4596(6)	15.5445(10)
α/°	99.036(4)	92.305(4)	90	100.256(3)	90	80.699(5)
β/°	112.556(5)	96.960(4)	104.227(4)	100.522(3)	96.975(3)	74.772(5)
γ/°	98.658(4)	113.162(5)	90	110.428(3)	90	78.370(5)
Unit cell volume/Å^3	1091.31(11)	1317.29(13)	2579.47(14)	1472.72(8)	3514.96(19)	1983.8(2)
Temperature/K	150(2)	150(2)	150(2)	150(2)	150(2)	150(2)
Space group	*P*1	*P*1	*P*21/*c*	*P*1	*C*2/*c*	*P*1
No. of formula units per unit cell, *Z*	2	1	4	2	4	2
Radiation type	Mo K_α	Mo K_α	Mo K_α	Cu K_α	Cu K_α	Mo K_α
Absorption coefficient, μ/mm^{-1}	0.685	0.573	0.589	4.683	3.997	0.405
No. of reflections measured	10198	11587	26141	10972	10226	16510
No. of independent reflections	5543	5714	5918	5777	3086	8278
R_{int}	0.0237	0.0273	0.0472	0.0223	0.0241	0.0265
Final R_1 values ($I > 2\sigma(I)$)	0.0403	0.0543	0.0358	0.0396	0.0618	0.0428
Final $wR(F^2)$ values ($I > 2\sigma(I)$)	0.0877	0.1022	0.0722	0.1019	0.1439	0.0896
Final R_1 values (all data)	0.0519	0.0788	0.0491	0.0423	0.0644	0.0622
Final $wR(F^2)$ values (all data)	0.0936	0.1136	0.0790	0.1046	0.1456	0.0985
Goodness of fit on F^2	1.031	1.032	1.046	1.060	1.095	1.030
CCDC number	1889216	1889219	1889217	1889214	1889218	1889215

Synthesis of $[Ca(S_2COEt)_2(HOEt)_3]$ (1): A suspension of calcium metal (1.23 g, 31 mmol) in ethanol (50mL) was stirred and heated under reflux for 4 hours, resulting in dissolution of the metal and evolution of hydrogen gas. The solution was filtered while still hot, through celite™. The filtered solution was allowed to cool to room temperature, resulting in the formation of colourless crystalline material. Carbon disulphide (4.61mL, 5.84 g, 75 mmol) was added to the reaction mixture, which immediately began to turn a pale yellow and the precipitate dissolve. After 2 hours of stirring, the volume of clear solvent was reduced until precipitation occurred. The precipitate was gently warmed back into solution. A yellow crystalline solid (**1**) was isolated after cooling to -28 °C (yield: 11.2g, 86%) (Found: C, 34:09%; H, 6:63%. Calc. for $C_{12}H_{28}Ca_1O_5S_4$: C, 34:26%; H, 6:71%). NMR δ^1H [C_6D_6]: 1.03 (t, J = 6.8 Hz, 9 H, C*H*$_3$CH$_2$OH), 1.14 (t, J = 7.2, 6 H, C*H*$_3$CH$_2$OCS$_2$), 2.26 (br s, 3H, CH$_3$CH$_2$O*H*), 3.57 (q, J = 6.8 Hz, 6 H, CH$_3$C*H*$_2$OH), 4.57 (q, J = 7.2, 4 H, CH$_3$C*H*$_2$OCS$_2$); δ^{13}C [C_6D_6]: 14.40 (*C*H$_3$CH$_2$OCS$_2$), 19.80 (*C*H$_3$CH$_2$OH), 59.35 (CH$_3$*C*H$_2$OH), 70.83 (CH$_3$*C*H$_2$OCS$_2$), 234.11 (CH$_3$CH$_2$O*C*S$_2$).

Synthesis of $[Ca(S_2COEt)_2(N,N'N''\text{-}Me_2NCH_2CH_2NMeCH_2CH_2NMe_2)]$ (2): Pentamethyldiethylenetriamine (pmdeta) (0.92 mL, 0.76 g, 4.4 mmol) was added to 30mL of toluene containing **1** (1.68 g, 4 mmol). The mixture was stirred overnight. The resulting pale cloudy yellow solution was heated gently, with stirring, to re-dissolve the product. The solution was filtered whilst hot through Celite™. Cooling of the solution to -28 °C resulted in formation of yellow forming plate-like crystals (**2**), which were isolated by filtration and washed with cold hexane (yield: 1.4 g, 77%). (Found: C, 38:47%; H, 7:54%; N9:48%. Calc. for $C_{15}H_{33}Ca_1N_3O_2S_4$: C,39:53%; H, 7:30%; N, 9:22%). NMR δ^1H [C_6D_6]: 1.10 (t, J =7.2 Hz, 6H, C*H*$_3$CH$_2$OCS$_2$), 1.52-1.62 (m, 2H, NC*H*$_2$), 1.69-1.93 (m, 4H, NC*H*$_2$), 2.18 (br s, 12H, NMe$_2$), 2.53 (s, 3H, NMe), 4.64 (q, J = 7.2 Hz, 4H, CH$_3$C*H*$_2$OCS$_2$); δ^{13}C [C_6D_6]: 14.3 (*C*H$_3$CH$_2$OCS$_2$), 43.9 (NMe$_2$), 46.3 (NMe), 55.2 (NCH$_2$CH$_2$N), 57.4 (NCH$_2$CH$_2$N), 69.4 (CH$_3$CH$_2$OCS$_2$), 233.6 (CH$_3$CH$_2$O*C*S$_2$).

Synthesis of $[Ca(S_2COEt)_2(Py)_3]$ (3): Pyridine (10mL, 9.78 g, 124 mmol) was added to 1.00g of **1** (2.38 mmol)dissolved in 20ml of toluene. The suspension was stirred for 2 hours. Heating results in a clear red/orange solution. The solution was filtered hot, through Celite™ and the volume of the filtrate was reduced in-vacuo. Cooling to room temperature resulted in the formation of large orange crystals of **3** (yield: 1.14 g, 92%). (Found: C, 48:47%; H, 4:96%; N, 8:15%. Calc. for $C_{21}H_{25}Ca_1N_3O_2S_4$: C, 48:53%; H, 4:85%; N, 8:08%). NMR δ^1H [C_6D_6]: 1.11 (t, J = 7.2 Hz, 6H, CH$_3$CH$_2$CS$_2$), 4.61 (q, J = 7.2 Hz, 4 H, CH$_3$CH$_2$OCS$_2$), 6.51-6.56 (m, 6H, C(3)*H* & C(5)*H* Py), 6.78-6.85 (m, 3H, C(4)*H* Py), 9.02-9.05 (m, 6H, C(2)*H* & C(6)*H* Py); δ^{13}C [C_6D_6]: 14.3 (*C*H$_3$CH$_2$OCS$_2$), 69.4 (CH$_3$*C*H$_2$OCS$_2$), 124.2 (*C*(3)H &

C(5)H Py), 137.1 (*C*(4)H Py), 150.2 (*C*(2)H & *C*(6)H Py), 233.88 ($CH_3CH_2OCS_2$).

Synthesis of [Ca(S_2COEt)$_2$(3-Me-Py)$_3$] (4): 3-methylpyridine (3-Me-Py) 10mL (9:57 g, 103 mmol) was added to 1.00g of **1** (2.38 mmol) in 20ml of toluene. The suspension was allowed to stir overnight, resulting in a cloudy deep red solution. Excess 3-Me-Py was removed in vacuo, leaving an orange semi-solid. The solid was dissolved 20mL toluene to form an orange solution. The solution was filtered hot, through Celite™ and the volume of the filtrate was reduced in-vacuo. Cooling to room temperature resulted in the formation of large red-orange crystals of **4** (yield: 0.95 g, 71%). (Found: C, 51:15%; H 5:73%; N, 8:15%. Calc. for $C_{24}H_{31}Ca_1N_3O_2S_4$: C, 51:31%; H, 5:56%; N, 7:48%). NMR δ^1H [C_6D_6]: 1.12 (t, J = 7.2 Hz, 6H,C*H*$_3$CH$_2$OCS$_2$), 1.71 (s, 9H, *Me*-Py), 4.61 (q, J = 7.2Hz, 4H, $CH_3CH_2OCS_2$), 6.58 (m, 3H, C(5)*H* Py), 6.73 (m, 3H, C(4)*H* Py), 8.92 (m, 6H, C(2)*H* & C(3)*H* Py); δ^{13}C [C_6D_6]: 14.3 (*C*H$_3$CH$_2$OCS$_2$), 18.1 (3-*Me*-Py), 69.3 ($CH_3CH_2CS_2$), 123.6 (*C*(5)H Py), 133.8 (*C*(3)Me Py), 137.5 (*C*(4)H Py), 147.5 (*C*(6)H Py), 150.7 (*C*(2)H Py), 233.75 ($CH_3CH_2OCS_2$).

Synthesis of [Ca(S_2COEt)$_2$(4-Me-Py)3] 5: 4-methylpyridine (4-Me-Py) 10mL (9:57 g, 103 mmol) was added to 1.00g of **1** (2.38 mmol) in 20ml of toluene. The suspension was allowed to stir overnight, resulting in a cloudy deep red solution. Excess 3-Me-Py was removed in vacuo, leaving an orange semi-solid. The solid was dissolved 20mL toluene to form an orange solution. The solution was filtered hot, through Celite™ and the volume of the filtrate was reduced in-vacuo. Cooling to room temperature resulted in the formation of large red-orange crystals of **5** (yield: 1.12 g, 84%). (Found: C, 52:98%; H, 6:13%; N, 6:39%. Calc. for $C_{24}H_{31}Ca_1N_3O_2S_4$: C, 51:31%; H, 5:56%; N, 7:48%). NMR δ^1H [C_6D_6]: 1.15 (t, J = 7.2Hz, 6H, C*H*$_3$CH$_2$OCS$_2$), 1.58 (s, 9H, *Me*-Py), 4.66 (q, J = 7.2Hz, CH$_3$C*H*$_2$OCS$_2$), 6.43 (dd, J^1 = 1.8 Hz, J^2 = 4.8Hz, 6H, C(3)*H* & C(5)*H* Me-Py), 9.00 (dd, J^1 = 1.8 Hz, J^2 = 4.8Hz, C(2)*H* & C(6)*H* Me-Py); δ^{13}C [C_6D_6]: 14.3 (*C*H$_3$CH$_2$OCS$_2$), 20.6 (*Me*-Py), 69.3 (CH$_3$*C*H$_2$OCS$_2$), 125. 1 (*C*(3)H & *C*(5)H, MePy), 148.7 (Me-*C*, Me-Py), 150.1 (*C*(2)H & *C*(6)H, Me-Py), 233.9 ($CH_3CH_2OCS_2$).

Synthesis of [Ca(S_2COEt)$_2$(4-Me$_2$N-Py)$_3$] 5: 4-Dimethylamino-pyridine (4-Me$_2$N-Py) 0.87g, (7.2 mmol) was added to 1.00g of **1** (2.38 mmol) in 20ml of toluene. The suspension was allowed to stir overnight, resulting in an orange solution. The solution was filtered hot, through Celite™ and the volume of the filtrate was reduced in-vacuo. Cooling to room temperature resulted in the formation of orange crystals of **6**. (yield: 1.34 g, 87 %). (Found: C, 49:95%; H, 6:49%; N,10:19%. Calc. for $C_{27}H_{40}Ca_1N_6O_2S_4$: C, 49:97%; H, 6:21%; N,12:95%). NMR δ^1H [C_6D_6]: 1.21 (t, J = 7.2Hz, 6H, C*H*$_3$CH$_2$OCS$_2$), 2.08 (s, 18H, 4-*Me*$_2$N-Py), 4.76 (q, J = 7.2Hz, CH$_3$C*H*$_2$OCS$_2$), 5.87 (dd, J^1 = 1.7Hz, J^2 = 5.3Hz, 6H, C(3)*H* & C(5)*H* 4-Me$_2$N-Py), 8.92 (dd, J^1 = 1.7Hz, J^2 = 5.3Hz, 6H, C(2)*H* & C(6)*H* 4-Me$_2$N-Py); δ^{13}C [C_6D_6]: 14.5 (*C*H$_3$CH$_2$OCS$_2$), 38.2 (4-*Me*$_2$N-Py), 68.4 ($CH_3CH_2OCS_2$), 106.6 (*C*(3)H & *C*(5)H 4-Me$_2$N-Py), 150.4 (*C*(2)H & *C*(6)H 4-Me$_2$N-Py), 154.5 (*C*(4)Me 4-Me$_2$N-Py), 234.1 ($CH_3CH_2OCS_2$).

Single Crystal X-ray Diffraction:

Experimental details relating to the single-crystal X-ray crystallographic studies for compounds **1**-**5** are summarised in Table 3. Single Crystal X-ray crystallography data were collected at 150 K on RIGAKU SuperNova Dual wavelength diffractometer equipped with an Oxford Cryostream, featuring a micro source with MoKα radiation (λ= 0.71073 Å) and CuKα radiation (λ= 1.5418 Å). Crystals were isolated from an argon filled Schlenk flask and immersed under oil before being mounted onto the diffractometer. All structures were solved by direct methods followed by full-matrix least squares refinement on F^2 using the WINGX-2014 suite of programs or OLEX2. All hydrogen atoms were included in idealized positions and refined using the riding model.[30]

Acknowledgments

This work was funded by the UK Engineering and Physical Sciences Research Council (EPSRC) via the Centre for Doctoral Training in New and Sustainable PV, EP/L01551X/1 (P.S.K.).

Keywords: Calcium Sulfide • Xanthate • Single source precursor • CVD • TGA

[1] a) R. Pandey, J. E. Jaffe, A. B. Kunz, Physical Review B 1991, **43**, 9228-9237; b) S. B. Kim, C. Yang, T. Powers, L. M. Davis, X. Lou, R. G. Gordon, Angew. Chem. Int. Ed., 2016, **55**, 10228-10233.

[2] R. Pandey, S. Sivaraman, J. Phys. Chem. Solids, 1991, **52**, 211-225.

[3] a) P. F. Smet, I. Moreels, Z. Hens, D. Poelman, Materials, 2010, **3**, 2834-2883; b) S.-H. Choi, C.-O. Park, H.-S. Park, S.-H. K. Park, S. J. Yun, J. Electrochem. Soc., 2004, 151.

[4] a) S. Hakamata, M. Ehara, H. Kominami, Y. Nakanishi, Y. Hatanaka, Appl. Surf. Sci., 2005, **244**, 469-472; b) D. Wauters, D. Poelman, R. L. Van Meirhaeghe, F. Cardon, J. Phys-Condens. Mat., 2000, **12**, 3901-3909; c) D. Poelman, R. Vercaemst, R. L. Van Meirhaeghe, W. H. Laflère, F. Cardon, J. Lumin., 1997, **75**, 175-181; d) I. V. F. Viney, B. Ray, J. W. Brightwell, B. W. Arterton, A. C. Wright, J. Mater. Sci.: Mater Electron., 1996, **7**, 305-308; e) M. Ando, Y. A. Ono, J. Cryst. Growth, 1992, **117**, 969-974; f) K. Świątek, M. Godlewski, L. Niinistö, M. Leskelä, Acta Phys. Pol. A, 1992, **82**, 769-772.

[5] a) Y. Zhao, F. T. Rabouw, T. v. Puffelen, C. A. v. Walree, D. R. Gamelin, C. de Mello Donegá, A. Meijerink, J. Am. Chem. Soc., 2014, **136**, 16533-16543; b) J. G. Zhang, P. C. Eklund, Z. L. Hua, L. G. Salamanca-Riba, M. Wuttig, P. K. Soltani, G. M. Storti, J. Mater. Res., 2011, **7**, 411-417; c) J. Wu, D. Newman, I. Viney, J Phys. D: Appl. Phys., 2004, **37**, 1371-1375; d) P. F. Smet, J. Van Gheluwe, D. Poelman, R. L. Van Meirhaeghe, J. Lumin., 2003, **104**, 145-150; e) J. Versluys, D. Poelman, D. Wauters, R. L. V. Meirhaeghe, J. Phys. Condens. Matter, 2001, **13**, 5709-5716; f) A. Kawasumi, T. Nakajima, H. Kominami, Y. Nakanishi, Y. Hatanaka, J. Cryst. Growth, 2000, **214-215**, 963-966; g) M. Ando, Appl. Phys. Lett., 1992, **60**, 2189-2191.

[6] a) Y. Charreire, R. D. Svoronos, I. Ascone, O. Tolonen, L. Niinistö, M. Leskelä, J. Electrochem. Soc., 1993, **140**, 2015-2019; b) Y. Charreire, O. Tolonen-Kivimäki, E. Nykänen, M. Leskelä, L. Niinistö, D. Bonnin, O. Heckmann, Thin Solid Films, 1994, **247**, 151-155.

[7] a) P. S. Dutta, K. M. Liotta, MRS Advances 2016, **1**, 3435-3440; b) W. H. Fan, X. Hou, W. Zhao, X. J. Gao, W. Zou, Y. Liu, Appl. Phys. A, 2001, **73**, 115-119; c) R. L. Nyenge, H. C. Swart, O. M. Ntwaeaborwa, Appl. Phys. A, 2016, **122**, 621-626; d) K. Świątek, M. Godlewski, L. Niinistö, M. Leskelä, J. Appl. Phys., 1993, **74**, 3442-3446.

[8] a) Y. S. Kim, S. J. Yun, J. Phys., Condens. Matter, 2004, **16**, 569-579; b) S. Lehto, L. Niinisto, I. Yliruokanen, Fresen J. Anal. Chem., 1993, **346**, 608-611.

[9] N. Yamashita, Y.-i. Sasaki, K. Nakamura, Japanese J. Appl. Phys., 1992, **31**, 2791-2797.

[10] P. Soininen, L. Niinistö, E. Nykänen, M. Leskelä, Appl. Surf. Sci., 1994, **75**, 99-105.

[11] J. M. Sun, G. Z. Zhong, X. W. Fan, C. W. Zheng, G. O. Mueller, R. Mueller-Mach, J. Appl. Phys., 1998, **83**, 3374-3378.

[12] Y. Zhao, F. T. Rabouw, C. d. M. Donegá, A. Meijerink, C. A. van Walree, Mater. Lett., 2012, **80**, 75-77.

[13] a) T. Hänninen, I. Mutikainen, V. Saanila, M. Ritala, M. Leskelä, J. C. Hanson, Chem. Mater., 1997, **9**, 1234-1240; b) J. Rautanen, M. Leskelä, L. Niinistö, E. Nykänen, P. Soininen, M. Utriainen, Appl. Surf. Sci., 1994, **82-83**, 553-558.

[14] A. P. Purdy, C. F. George, Main Group Met. Chem., 1996, **1**, 229-240.

[15] a) I. Y. Ahmet, M. S. Hill, A. L. Johnson, L. M. Peter, Chem. Mater., 2015, **27**, 7680-7688; b) X. Hou, K. L. Choy, Chem. Vap. Deposition, 2006, **12**,

583-596; c) C. E. Knapp, C. J. Carmalt, Chem. Soc. Rev., 2016, **45**, 1036-1064; d) P. Marchand, I. A. Hassan, I. P. Parkin, C. J. Carmalt, Dalton Trans., 2013, **42**, 9406-9422; e) T. Wildsmith, M. S. Hill, A. L. Johnson, A. J. Kingsley, K. C. Molloy, Chem. Commun., 2013, **49**, 8773-8775.

[16] R. Helbing, H. Birecki, S. A. DiCarolis, R. S. Feigelson, R. Hiskes, J. Cryst. Growth, 1995, **146**, 599-603.

[17] M. Tammenmaa, H. Antson, M. Asplund, L. Hiltunen, M. Leskelä, L. Niinistö, E. Ristolainen, J. Crys. Growth, 1987, **84**, 151-154.

[18] K. Kunze, L. Bihry, P. Atanasova, M. J. Hampden-Smith, E. N. Duesler, Chem. Vap. Deposition, 1996, **2**, 105-108.

[19] D. Barreca, A. Gasparotto, C. Maragno, R. Seraglia, E. Tondello, A. Venzo, V. Krishnan, H. Bertagnolli, Appl. Organomet. Chem., 2005, **19**, 1002-1009.

[20] a) M. A. Buckingham, A. L. Catherall, M. S. Hill, A. L. Johnson, J. D. Parish, Cryst. Growth Des., 2017, **17**, 907-912; b) D. Barreca, A. Gasparotto, C. Maragno, R. Seraglia, E. Tondello, A. Venzo, V. Krishnan, H. Bertagnolli, Appl. Organomet. Chem., 2005, **19**, 59-67.

[21] J. Akhtar, M. Afzaal, M. A. Vincent, N. A. Burton, I. H. Hillier, P. O'Brien, Chem. Commun., 2011, **47**, 1991-1993.

[22] A. L. Johnson, M. S. Hill, G. Kociok-Köhn, K. C. Molloy, A. L. Sudlow, Inorg. Chem. Commun., 2014, **49**, 8-11.

[23] N. Alam, M. S. Hill, G. Kociok-Köhn, M. Zeller, M. Mazhar, K. C. Molloy, Chem. Mater., 2008, **20**, 6157-6162.

[24] E. R. T. Tiekink, I. Haiduc, Prog. Inorg. Chem., 2005, 127-319.

[25] a) I. K. Bezougli, A. Bashall, M. McPartlin, D. M. P. Mingos, J. Chem. Soc., Dalton Trans., 1998, 2671-2678; b) I. K. Bezougli, A. Bashall, M. McPartlin, D. M. P. Mingos, J. Chem. Soc., Dalton Trans., 1998, 2665-2670.

[26] J. M. Clark, G. Kociok-Köhn, N. J. Harnett, M. S. Hill, R. Hill, K. C. Molloy, H. Saponia, D. Stanton, A. Sudlow, Dalton Trans., 2011, **40**, 6893-6900.

[27] G. Reck, R. Becker, Acta Crystallogr. C, 2004, **60**, m134-m136.

[28] Y. Tang, L. N. Zakharov, W. S. Kassel, A. L. Rheingold, R. A. Kemp, Inorg. Chim. Acta, 2005, **358**, 2014-2022.

[29] A. J. Vreugdenhil, S. H. R. Brienne, I. S. Butler, J. A. Finch, R. D. Markwell, Spectrochim. Acta A, 1997, **53**, 2139-2151.

[30] L. J. Farrugia *J. Appl. Crystallogr.*, 2012, **45** , 849-854.

Entry for the Table of Contents

FULL PAPER

CaS, is a potentially important component in semiconductor materials with applications in wide range of thin-film luminescent displays. Here, we describe our initial studies into the development of a family of Ca-Xanthate single source precursors of the general form $[\{L\}_xCa\{S_2COEt\}_2]$ ($\{L\}_x$ are nitrogen containing ligands). The solid state structures, thermal profiles, and initial decomposition studies of these new precursors are described.

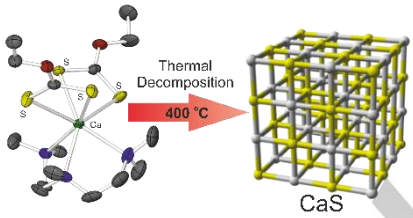

Key Topic* Single Source Precursors, Calcium Sulfide, Xanthates

*P. S. Kubiak, P. J. Cameron, G. Kociok-Köhn and A. L. Johnson.**

Page No. – Page No.

Single Source Precursors for Calcium Sulfide (CaS) Deposition